Inorganica Chimica Acta, 71 (1983) 217–226

X-ray Structure of *Trans*-tetrakis(pyrazole)bisisothiocyanatomanganese(II) and its Magnetic, Spectral and Thermal Properties

PAAVO LUMME, ILPO MUTIKAINEN and EVA LINDELL

Department of Inorganic Chemistry, University of Helsinki, SF-00100 Helsinki 10, Finland

Received September 3, 1982

The crystal structure of trans-*tetrakis(pyrazole)-bisisothiocyanatomanganese(II), $(C_3H_4N_2)_4(NCS)_2$-Mn(II), was determined from single-crystal three-dimensional X-ray diffractometer data. The compound crystallizes as almost colourless cubes in the space group* C2/c. *The unit cell parameters are* a = *11.485(4),* b = *12.513(4),* c = *14.554(11)* Å *and* β = *105.04(5)°,* Z = *4. The structure was solved by Patterson and Fourier syntheses and the full-matrix least-squares refinement of 877 unique reflections gave the final value of* R = *0.040. There are discrete molecules in the crystal. The structure consists of centrosymmetric complex units in which the central Mn(II) ion is in an octahedral planar arrangement of two N(1) coordinated and two N(3) coordinated pyrazole molecules occupying the equatorial sites at distances of 2.247(5) and 2.237(5)* Å, *respectively. The apical sites are occupied by two symmetry-related N(5) coordinated isothiocyanato anions at 2.202(6)* Å *and in* trans-*positions with respect of each other, as are the opposite pyrazole molecules in the basal plane. The neighboring pyrazole planes are tilted toward each other and the basal plane. The structure is held together primarily through hydrogen bonds approximately in* b- *and* c-*directions from S(1) atom of each isothiocyanato anion to two pyrazole NH groups of the neighboring molecule and the interaction of the stacked parallel pyrazole rings, especially in the* c-*direction.*

The paramagnetic susceptibility follows the Curie-Weiss law at temperatures from 93 to 298 K. The IR spectrum shows M–N bands. The reflectance spectrum has one band at 23 260 cm^{-1} assigned to the $^6A_{1g} \rightarrow {}^4T_{2g}$ transition. The TG curve points to two kinds of pyrazole with different bonding strengths in the structure.

Introduction

The two possible five-membered diazole cyclic compounds, imidazole and pyrazole, and their metal complexes have been objects of intensive investigations already during three decades [1], mainly because of physiologically or medically important biological compounds and process systems [2].

Usually the complexes between pyrazole and metal ions of the first transition metal series are of the form $M(Hpz)_nX_m$, where M = metal, Hpz = pyrazole and X = anion [1]. The pyrazole ring is coordinated to the metal through 'the pyridine nitrogen', $\geqslant$ N [3]. As in the case of imidazole also the second nitrogen atom, the socalled 'pyrazole nitrogen', $>\overline{N}$–H participates to hydrogen bonds in the complexes [4]. Such mononuclear compounds are usually formed by direct reaction between pyrazole and metal salts in neutral or weakly acid solutions [1]. Instead, in alkaline conditions polymers, $[M(Pz)_2]_n$, where Pz = deprotonated pyrazole, are formed [1]. The geometry of the pyrazole ligand allowes it to act as a bridge between two metal atoms [1, 5]. The structure may then be polymeric or also binuclear, when two pyrazole ligands are bonded to two metal atoms [1].

Pyrazole is easily substituted at positions 3 and 5. A substituent at position 3 of the pyrazole ring causes a steric hindrance, when six such ligands have not enough space to coordinate to one metal atom [1]. On the contrary at position 5 substituted pyrazole ligand is said to be able to form such a complex [1], $M(5L\text{-}Hpz)_6^{n+}$, although the crystal structure of no such compound has been elucidated. Only four of the extensively studied 3,5-dimethylpyrazole ligands are coordinated to the same metal atom [1]. On the other hand a substituent at the position 4 affects not the coordination ability of the ligand, but *e.g.* 4-methyl-pyrazole behaves as the unsubstituted pyrazole molecule [1].

A literature search showed that the crystal structures of about 35 complexes of pyrazole or substituted pyrazoles with the metals of the first transition series have been solved so far, most of them nickel, cobalt and copper complexes. The majority of these belong to the monoclinic or triclinic systems. The coordination number of the metal ion varies in these complexes from 2 to 6, as in imidazole complexes. The most frequent coordination number is undoubtedly six, and a distorted octahedron is the most general coordination polyhedron.

In general the crystal structure determinations have been made after the complexes have been

0020-1693/83/0000-0000/$03.00

studied first from a magnetochemical viewpoint, and with several spectroscopic methods [1].

Several manganese(II) complexes of pyrazole and its derivatives are reported to have been prepared, including $Mn(Hpz)_4(NCS)_2$ [6], and studied with different physical methods [1] but the crystal structure of only two has been solved [7]. The present paper tries to give further information in this respect. The prepared *trans*-tetrakis(pyrazole)bisisothiocyanato-manganese(II) was also studied with respect to magnetic susceptibility, IR and reflectance spectra and thermal behaviour; the results are reported below and discussed.

Experimental

Reagents, Syntheses and Analyses

For preparation of the $Mn(C_3H_4N_2)_4(NCS)_2$ complex 7.92 g (0.04 mol) $MnCl_2 \cdot 4H_2O$ (p.a., Merck) in 10 cm^3 hot water was added with stirring into a hot aqueous solution (30 cm^3) of 2.73 g (0.04 mol) pyrazole (purum, Fluka AG) and 19.44 g (0.2 mol) KSCN (p.a., Merck). The mixture was allowed to evaporate slowly and stand overnight. The separated colourless cubical shaped crystals were filtered on a sinter, recrystallized from hot water (2% in KSCN) and stored in a desiccator. The other reagents used were of guaranteed quality. For analysis manganese was determined by EDTA titration [8], sulphur gravimetrically as silver thiocyanate [8], and other elements by micro combustion analyses. *Anal.* Found: C, 37.44; H, 3.50; N, 31.50; S, 14.38; Mn, 12.13. Calcd. for $C_{14}H_{16}N_{10}S_2Mn$: C, 37.92; H, 3.64; N, 31.59; S, 14.46; Mn, 12.39%.

Data Collection and Structure Determination

Weissenberg photographs established the space group as monoclinic *Cc* or *C2/c* from systematic absences $h + k = 2n + 1$ and $l = 2n + 1$. The space group *C2/c* was assigned on the basis of the complete structure analysis.

Powder diffraction data were obtained from photographs taken on a Guinier-Hägg camera (Philips) using 19.7 per cent of CaF_2 ($a = 5.4638$ Å [9]) as an internal standard and $CuK\alpha_1$ radiation ($\lambda = 1.5405$ Å). The observed and calculated d spacings (Å) and observed relative intensities are given in Table I and the corresponding unit cell dimensions are in Table II.

TABLE I. Observed and Calculated d Spacings (Å) and Estimated Relative Intensities for $Mn(C_3H_4N_2)_4(NCS)_2$.

hkl	d_o	d_c	I/I_o	hkl	d_o	d_c	I/I_o
110	7.846	7.845	s	202	3.392	3.393	m
002	7.028	7.028	m	$\bar{1}33$	3.286	3.287	w
$\bar{1}12$	6.605	6.604	m	$\bar{2}42$	2.724	2.724	w
020	6.264	6.258	vw	223	–	2.571	–
200	5.034	5.034	w	$\bar{1}16$	2.518	2.518	vw
$\bar{2}21$	4.207	4.207	m	400	–	2.517	–
$\bar{2}22$	4.148	4.148	m	$\bar{4}21$	2.490	2.490	vw
$\bar{2}04$	3.885	3.887	m	$\bar{2}44$	2.438	2.437	w
023	3.749	3.750	m	420	2.335	2.335	vw
$\bar{1}32$	3.674	3.676	w	$\bar{5}12$	2.207	2.206	vw
$\bar{3}12$	3.659	3.659	w				
$\bar{3}13$	3.542	3.543	w				
113	3.490	3.489	w				

The crystal selected for intensity data collection had the dimensions of 0.40 × 0.40 × 0.40 mm^3. The unit cell parameters (Table II) were determined by least-squares treatment of the adjusted angular settings of 12 reflections measured on a Syntex $P2_1$ diffractometer. The intensity measurements were carried out at room temperature (23 ± 2 °C) with graphite-monochromated MoKα radiation and the $\theta-2\theta$ scan technique. The scan rate varied from 2.0 to 29.3° min^{-1}, depending on the number of counts measured in a fast preliminary scan through the peak. A set of 1961 unique reflections was obtained from the 2037 reflections measured up to the maximum value of $2\theta = 50°$. 877 reflections with $I > 3\sigma(I)$ were considered as observed and used in the refinement. Two strong reflections monitored periodically exhibited no significant variation of intensity. The intensities were corrected for Lorentz and polarization effects but corrections for absorption and extinction were considered unnecessary.

In the space group *C2/c* with $Z = 4$ the Mn atoms must lie on special positions. On the basis of three dimensional Patterson synthesis Mn was situated at 0.25, 0.25, 0.5 and the sulphur atom of the thiocyanate group at 0.3963, 0.1342, 0.080. The rest of

TABLE II. Crystal Data for $Mn(C_3H_4N_2)_4(NCS)_2$.

Monoclinic *C2/c* (No. 15)			
(Syntex $P2_1$)	(Powder)	F.W.	= 443.4
a = 11.485(4) Å	11.477(1) Å	Z	= 4
b = 12.513(4)	12.515(2)	d_m	= 1.46 Mg m^{-3}
c = 14.554(11)	16.022(4)	d_c	= 1.46
β = 105.04(5)°	118.69(2)°	λ(MoKα)	= 0.71609 Å
V = 2020(2) Å^3	2019(3) Å^3	μ(MoKα)	= 0.86 mm^{-1}

the non-hydrogen atoms were found during successive Fourier syntheses. With anisotropic temperature factors for the non-hydrogen atoms, a difference map calculated after full-matrix refinement revealed the positions of all four hydrogen atoms. Full-matrix least-squares refinement with all non-hydrogen atoms as anisotropic and hydrogen atoms with uniform isotropic thermal parameters ($U = 0.05$ Å^2) led to $R = \Sigma||F_o| - |F_c||/|F_o| = 0.040$ and $R_w = (\Sigma w(|F_o| - |F_c|)^2/\Sigma w|F_o|^2)^{1/2} = 0.043$, where $w = 1/\sigma(F_o^2)$. After the last cycle the average shift/error was 0.044 and maximum shift/error 0.292. A final difference map was practically featureless.

Scattering factors were from Cromer and Mann [10] and the anomalous dispersion correction was applied [11]. All calculations were performed on a Univac 1108 computer with X-RAY 76 by Stewart [12]; for planes a program MPLN by Truter [13a] was used, and for powder data the program PIRUM [13b].

Physical Measurements

Magnetic susceptibility measurements of the powdered compound (particle size 60–140 mesh) were done on a variable-temperature Gouy balance system (Newport Instruments Ltd.) at ten degree intervals in the temperature range 93.2–293.2 K. The system was calibrated with copper(II) sulphate pentahydrate [14]. The magnetic susceptibility data are mean values from measurements on four magnetic fields. The calculated diamagnetic correction used was -234.6×10^{-6} e.m.u.

Infrared spectra were recorded in KBr disks (1.5 mg of the compound: 200 mg of KBr) on a Perkin-Elmer Grating Infrared Spectrophotometer Model 577.

Reflectance spectra were recorded on a Beckman DK-2A spectrophotometer using a filter paper treated with a paraffin oil paste of the studied compound.

TG curves were run on a Perkin-Elmer TGS-1 Thermobalance. The sample amount was about 2 mg, the cups used from Al, the heating rate 10 °C min^{-1} and the atmosphere dynamic nitrogen, with a flow of about 35 cm^3 min^{-1}.

Densities of the crystals were determined by the flotation method in toluene-CCl_4 mixtures.

Results and Discussion

Description of the Structure

The fractional atomic coordinates and the equivalent values of the anisotropic temperature factor coefficients (U_{eq}) for non-hydrogen atoms are listed in Table III and the calculated fractional coordinates for the hydrogen atoms in Table IV. A list of observed and calculated structure factors and anisotropic thermal parameters is available on request from the Editor.

TABLE III. Fractional Atomic Coordinates ($\times 10^4$) and Equivalent Values of the Anisotropic Temperature Factor Coefficients[a] ($\times 10^4$) of Non-hydrogen Atoms with e.s.d. s in Parentheses.

Atom	x	y	z	U_{eq} (Å^2)
Mn	2500(0)	2500(0)	5000(0)	337(8)
N(1)	2707(4)	1863(4)	6477(3)	370(33)
N(2)	3380(5)	1016(5)	6829(5)	500(45)
N(3)	3764(5)	3815(4)	5652(4)	427(37)
N(4)	3515(6)	4873(5)	5609(4)	556(47)
N(5)	4023(5)	1483(4)	4892(4)	513(38)
C(1)	3460(7)	881(7)	7777(6)	578(58)
C(2)	2812(6)	1667(6)	8050(5)	516(51)
C(3)	2367(6)	2262(5)	7228(5)	463(51)
C(4)	4493(9)	5451(7)	6052(6)	680(66)
C(5)	5342(10)	4753(10)	6381(7)	770(79)
C(6)	4916(7)	3737(7)	6143(5)	553(56)
C(7)	4845(6)	1417(5)	4592(4)	388(40)
S(1)	6029(2)	1341(2)	4137(1)	567(13)

[a] $U_{eq} = \frac{1}{3} \sum_i \sum_j U_{ij} a_i^* a_j^* \vec{a}_i \cdot \vec{a}_j$ [16].

TABLE IV. Fractional Atomic Coordinates ($\times 10^3$) for Hydrogen Atoms with e.s.d. s in Parentheses.

Atom	x	y	z
H(1)	362(5)	61(5)	650(4)
H(2)	379(5)	22(5)	798(4)
H(3)	278(5)	186(4)	875(4)
H(4)	197(5)	298(5)	711(4)
H(5)	274(5)	517(5)	535(4)
H(6)	451(5)	625(5)	618(4)
H(7)	599(5)	480(6)	661(5)
H(8)	527(5)	310(4)	617(4)

The bond lengths and angles are shown in Table V. The least-squares planes through the pyrazole's N atoms coordination sphere around the Mn atom and of the neighboring pyrazole rings and distances of the atoms from the planes are given in Table VI. The hydrogen bond data are collected in Table VII. An ORTEP drawing [15] of the complex showing the molecular geometry and atom numbering scheme is presented in Fig. 1. The molecular packing and hydrogen bond directions in the unit cell are seen in Fig. 2.

The Mn Coordination Sphere

The asymmetric unit includes a half of the Mn atom, one isothiocyanato ion and two pyrazole molecules. According to this the Mn atom is hexacoordinated to four pyrazole molecules at N(1), N(1)^i, N(3) and N(3)^i and to two isothiocyanato anions at N(5) and N(5)^i atoms. The Mn coordination sphere is a slightly distorted octahedron, with four pyrazole molecules in the equatorial positions and the

TABLE V. Bond Distances (Å) and Angles (°) with e.s.d. s in Parentheses.

Symmetry code

Superscript

None	x	y	z
i	0.5 − x	0.5 − y	1 − z

(a) Manganese coordination sphere

Mn–N(1)	2.247(5)	Mn–N(1)–C(3)	131.5(4)
Mn–N(3)	2.237(5)	Mn–N(1)–N(2)	123.8(4)
Mn–N(5)	2.202(6)	Mn–N(3)–N(4)	126.5(4)
		Mn–N(3)–C(6)	128.2(5)
(Uncoordinated)		Mn–N(5)–C(7)	145.2(5)
Mn–N(2)	3.187(6)	N(1)–Mn–N(3)	87.7(2)
Mn–N(4)	3.229(6)	N(1)–Mn–N(3)^{i}	92.3(2)
Mn–C(3)	3.298(5)	N(1)–Mn–N(5)	88.5(2)
Mn–C(6)	3.235(7)	N(1)–Mn–N(5)^{i}	91.5(2)
		N(3)–Mn–N(5)	90.9(2)
		N(3)–Mn–N(5)^{i}	89.1(2)

(b) Pyrazole ligands

N(1)–N(2)	1.332(7)	N(1)–N(2)–C(1)	111.4(6)
N(2)–C(1)	1.369(11)	N(2)–C(1)–C(2)	107.9(6)
C(1)–C(2)	1.353(11)	C(1)–C(2)–C(3)	104.1(7)
C(2)–C(3)	1.389(10)	C(2)–C(3)–N(1)	112.3(6)
C(3)–N(1)	1.347(9)	C(3)–N(1)–N(2)	104.2(5)
N(3)–N(4)	1.353(8)	N(3)–N(4)–C(4)	111.3(6)
N(4)–C(4)	1.351(11)	N(4)–C(4)–C(5)	105.4(8)
C(4)–C(5)	1.304(14)	C(4)–C(5)–C(6)	110.1(7)
C(5)–C(6)	1.375(14)	C(5)–C(6)–N(3)	107.8(7)
C(6)–N(3)	1.334(8)	C(6)–N(3)–N(4)	105.4(5)

(c) Isothiocyanato ion

N(5)–C(7)	1.141(9)	N(5)–C(7)–S(1)	178.7(5)
C(7)–S(1)	1.663(7)		

(d) Hydrogen atoms

N(2)–H(1)	0.79(7)	N(1)–N(2)–H(1)	123(4)
C(1)–H(2)	0.93(5)	C(1)–N(2)–H(1)	125(4)
C(2)–H(3)	1.06(6)	N(2)–C(1)–H(2)	111(4)
C(3)–H(4)	1.00(5)	C(2)–C(1)–H(2)	140(4)
		C(1)–C(2)–H(3)	127(3)
		C(3)–C(2)–H(3)	128(3)
		C(2)–C(3)–H(4)	132(3)
		N(1)–C(3)–H(4)	114(3)
N(4)–H(5)	0.95(5)	N(3)–N(4)–H(5)	125(3)
C(4)–H(6)	1.01(6)	C(4)–N(4)–H(5)	124(3)
C(5)–H(7)	0.73(6)	N(4)–C(4)–H(6)	126(3)
C(6)–H(8)	0.89(5)	C(5)–C(4)–H(6)	128(3)
		C(4)–C(5)–H(7)	133(6)
		C(6)–C(5)–H(7)	116(5)
		C(5)–C(6)–H(8)	133(4)
		N(3)–C(6)–H(8)	118(3)

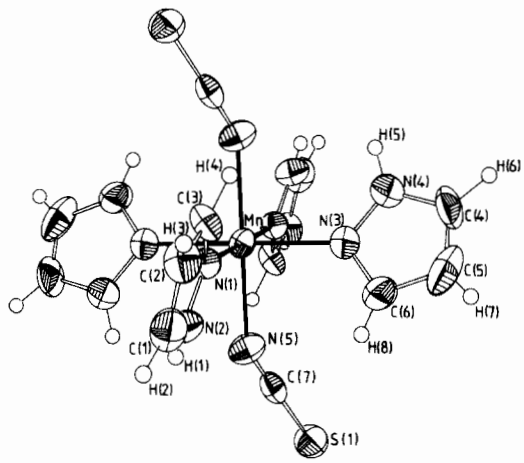

Fig. 1. An ORTEP drawing of the $Mn(C_3H_4N_2)_4(NCS)_2$ complex (with 295 K parameters) showing the molecular geometry and atom numbering scheme. Thermal ellipsoids are drawn at 50% probability level for the non-hydrogen atoms.

two isothiocyanato anions occupying the axial sites. The Mn–N(1) length is 2.247(5), the Mn–N(3) length 2.237(5) Å and the angle N(1)–Mn–N(3) is 87.7(2)°. The Mn–N(5) length is 2.202(6) Å and the angles N(5)–Mn–N(1) and N(5)–Mn–N(3) are 88.5(2) and 90.9(2)°, respectively. Because of the centro symmetry, the Mn atom lies in the equatorial plane.

TABLE VI. Analyses of the Most Significant Planes with Displacements of Each Atom. The e.s.d. s in Parentheses.

PLANE	N(1)N(3)N(11)N(31)	9.48603x − 6.97046y − 4.33609z = −1.53915[a]
	N(1), N(3), N(11), N(31), Mn all 0.000(0)	
PLANE	N(1)N(2)C(1)C(2)C(3)	8.98831x + 7.23386y + 0.28955z = 3.97020
	N(1) −0.002(6), N(2) 0.000(6), C(1) 0.002(7), C(2) −0.003(7), C(3) 0.003(6)	
PLANE	N(3)N(4)C(4)C(5)C(6)	−5.95920x − 0.75726y + 13.94480z = 5.35316
	N(3) −0.003(6), N(4) 0.005(6), C(4) −0.004(9), C(5) 0.002(8), C(6) 0.001(7)	

[a] x, y, z are the fractional coordinates in direct space.

TABLE VII. Distances and Angles in Interactions of the Type D–H···A.

D	H	A	D–H (Å)	D···A (Å)	H···A (Å)	D–H···A (°)
N(2)[a]	H(1)	S(1)	0.79(7)	3.41(2)	2.68(6)	154
N(4)[b]	H(5)	S(1)	0.95(5)	3.60(9)	2.71(8)	156

Symmetry position of atom D: (a) $-x+1, -y, -z+1$; (b) $x+\frac{1}{2}, y-\frac{1}{2}, z$.

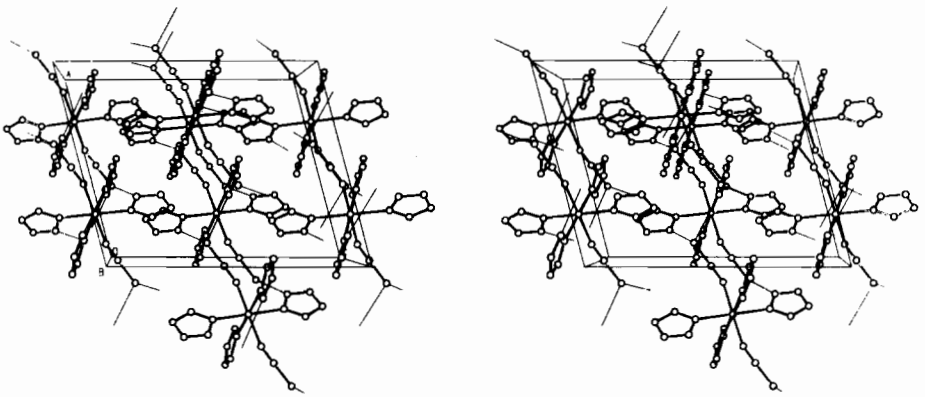

Fig. 2. Stereo arrangement of the molecules in a unit cell viewed down B.

TABLE VIII. Comparison of the M–X, M–N(1) and M–N(3) Bond Lengths (Å) in Some Pyrazole Complexes.[a]

Compound	$Mn(HPz)_4(NCS)_2$	$[Mn(HPz)_2Cl_2]_\infty$	$Mn(MPz)_4Br_2$	$Ni(HPz)_4(ONO)_2$	$Ni(HPz)_4Cl_2$
Reference	[This work]	[7b]	[7a]	[17]	[18]
M–X	2.202(6)	2.592(2), 2.594(2)	2.727(2)	2.09(1), 2.14(1)	2.507(1)
M–N(1)	2.247(5)	2.201(3)	2.256(3)	2.097(4)	2.097(2)
M–N(3)	2.237(5)	2.201(3)	2.243(3)	2.079(4)	2.087(3)

Compound	$Ni(HPz)_4Br_2$	$Ni(HPz)_6(NO_3)_2$	$Co(DMPPz)_2(NCS)_2$	$Cu(HPz)_4Cl_2$
Reference	[19]	[20]	[21]	[22]
M–X	2.682(1)		1.947(6), 1.962(6)	2.840(1)
M–N(1)	2.101(4)	2.125(3)	2.036(5)	2.024(1)
M–N(3)	2.080(5)	2.125(3)	2.022(6)	2.009(1)

[a]MPz = 5-Methylpyrazole, DMPPz = 3,5-Dimethyl-1-phenylpyrazole.

The Mn–ligand bond lengths agree well with those found in other Mn complexes, though the Mn–N(5) length is rather short for a hexacoordinated Mn complex as seen in Table VIII, where M–ligand bonds in several pyrazole complexes are compared. From the values it is seen that the octahedron in this complex is less distorted from its ideal geometry than is the case in other Mn complexes [7].

The opposite pyrazole molecules in the basal plane around the Mn atom are in *trans*-arrangement in respect of each other. Their planes are parallel, but tilted to neighboring ring and the equatorial plane. The N(1) and N(3) containing pyrazole ring planes are in 72.3(2)° and 117.9(3)° angles to the basal plane, respectively, and to each others in 104.1(3)° angle. The reason lies obviously in the intermolecular hydrogen bonds causing the inclination of the corresponding pyrazole rings toward S(1) atoms.

The Pyrazole Ligand Structure

The pyrazole rings are planar within e.s.d. values, but are deformed slightly differently by coordination to the Mn atom as shown by the atom distances from the planes in Table VI. The N(1) coordination alters the pyrazole ring geometry by shortening the N(1)–N(2) bond length, lengthening the other bonds, closing the N(1)–N(2)–C(1) and C(1)–C(2)–C(3) angles and opening the others in the ring as compared with the uncoordinated pyrazole molecule [23]. On the other hand the N(3) coordination changes the

pyrazole ring geometry more radically by shortening the C(4)–C(5) bond length to 1.304(14) Å and opening the C(4)–C(5)–C(6) and C(6)–N(3)–N(4) angles to 110.1(7) and 105.4(5)°, respectively. In the uncoordinated pyrazole the values are 1.346(13) Å, 105.2(6) and 103.6(5)°, respectively [23]. All other bonds are lengthened and angles closed (Table V).

The bond lengths in N(1) coordinated pyrazole rings are very similar as compared with those in other pyrazole complexes [7b], whereas the bond angles differ more. In the case of N(3) coordinated pyrazole rings the situation is stressed. The reason for these differences is obviously (in part) the two intermolecular hydrogen bonds described above.

The Isothiocyanato Ion

The two isothiocyanato anions are coordinated through the N(5) atoms to Mn occupying the axial sites. They are situated in *trans*-arrangement in respect of each other. This confirms the earlier conclusion obtained on the basis of the infrared spectrum [6].

The anion is not perfectly linear, the N(5)–C(7)–S(1) angle being 178.7(5)°. This is comparable with that (178.3(1.2)°) of KNCS [26c], whereas the bond lengths N(5)–C(7) and C(7)–S(1) are a little shorter (1.149(14) and 1.689(13) Å, respectively, in KNCS) [26c].

Molecular Arrangement and Hydrogen Bond System

The structure determining property is that the Mn atoms form rows in *b*-direction. The neighboring chains are displaced by $\frac{1}{2}00$, $-\frac{1}{2}00$, $00\frac{1}{2}$ and $00-\frac{1}{2}$. In this respect the structure is similar to that of $[Mn(Hpz)_2(Cl)_2]_\infty$ [7b]. The plane defined by the Mn and four surrounding pyrazole N atoms (the equatorial or basal plane) is, however, not perpendicular to *xz*-plane, but 123.9(1)° angle to it. Further, the plane N(1)–N(5)–N(1)^i–N(5)^i is nearly perpendicular to the equatorial coordination plane, the angle between them being 89.1(1)°. Instead of that the angle between the plane N(3)–N(5)–N(3)^i–N(5)^i and the basal plane is 91.5(1)°. The bond Mn–N(1) is not in the plane of the N(1) pyrazole ring, but forms an angle of 7.1° with it. The bond Mn–N(3), however, lies almost in the plane of the N(3) pyrazole ring, the angle between them being only 1.1°. The angle between the mentioned two non-basal planes is 92.4(1)°.

The pyrazole rings form columns approximately along the [001], [−110] and [110] directions, although the overlap is far from perfect. The rings in the columns are parallel with each other. The distances between the ring planes are approximately 3.64, 8.49 and 8.49 Å, respectively. The Mn atoms and isothiocyanato ions lie between these pyrazole columns. The columnar network is primarily held together by hydrogen bonds between the two H atoms (H(1) and H(5)) of the N(2) and N(4) atoms of the pyrazole rings and S(1) atoms of the isothiocyanato ions of neighboring molecular units (Table VII). A further stabilization of the crystal structure is obviously achieved through π electron system interactions of the stacked pyrazole rings in *c*-direction. As is commonly found in the crystal structures of pyrazole complexes [7], the stacking of the pyrazoles is not very extensive.

The hydrogen bond data in Table VII as compared with those reported [7b] for $[Mn(Hpz)_2(Cl)_2]_\infty$ implie the N(2)^a–H(1)···S(1) and N(4)^b–H(5)···S(1) hydrogen bonds in the present complex to be little stronger than the N–H···Cl hydrogen bonds in the mentioned compound. They are, however, weaker than N–H···X(halogen) hydrogen bonds in general [7b].

From the two intermolecular hydrogen bonds the N(4)^b–H(5)···S(1) bond (Table VII) is considered to be weaker on the basis of the longer bond length and, because it closes only slightly the Mn–N(3)–N(4) angle compared to the Mn–N(3)–C(6) angle. The stronger, shorter N(2)^a–H(1)···S(1) hydrogen bond causes a considerable diminution of the Mn–N(1)–N(2) angle compared with that of Mn–N(1)–C(3) (Table V). These circumstances are significant for the thermal behaviour of the compound as seen later.

Magnetic Behaviour

The molar paramagnetic susceptibility corrected for diamagnetism with Pascal's constants [24] follows the Curie-Weiss law: $X'_M = 4.812/(T + 4.98)$ in the temperature range T = 93.2 – 293.2 K. μ_{eff} varies, respectively, between 6.06 and 6.18 (B.M.) in accordance with the weakness of the complex and its spin-free character.

As seen from Table IX and Fig. 3 the magnetic susceptibility depends from absolute temperature practically linearly within the used temperature range, but μ_{eff} is almost constant. The μ_{eff} values are a little higher than the spin-only value 5.92 (B.M.) for manganese(II) ion [24] and imply obviously a weak orbital contribution. The results are, however, in agreement with the octahedral coordination around the manganese(II) ion and its high spin d^5 ($t_{2g}^3 e_g^2$) electron configuration. Measurements of magnetic susceptibility at temperatures under 90 K would probably reveal Curie-Weiss law escaping behaviour, but it would involve single crystal measurements best made on a vibrating magnetometer.

Infrared and Reflectance Spectra

The absorption band values of the IR spectra of pyrazole and the complex are collected in Table X. In addition to the ligand spectrum comparison also the bands of KSCN taken in KBr disks are presented.

The strong bands at 3430 and 3320 cm^{-1} in the complex spectrum are assigned to ν(NH) stretching

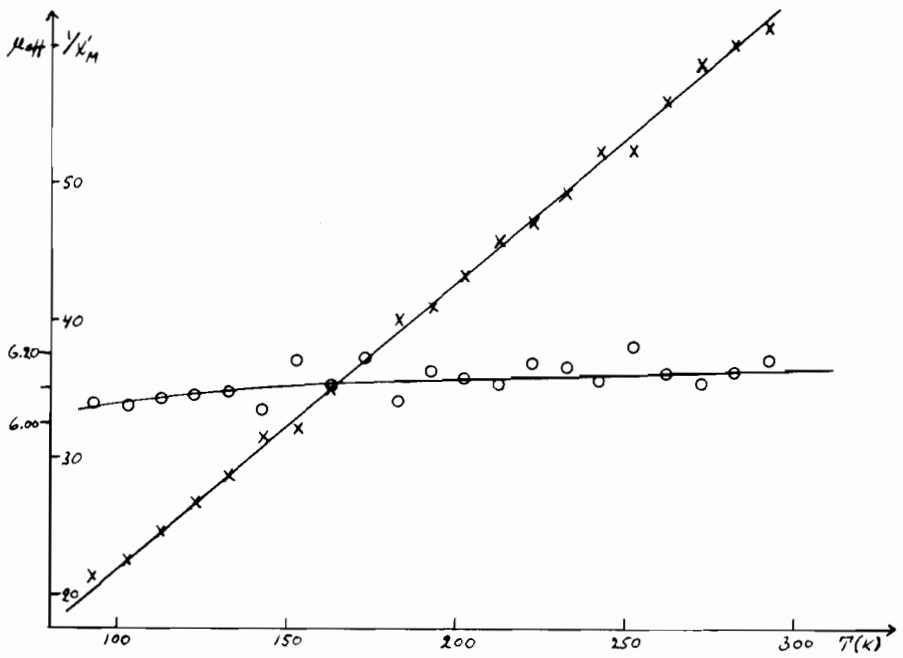

Fig. 3. $1/X'_M$ and μ_{eff} against absolute temperature for $Mn(C_3H_4N_2)_4(NCS)_2$.

TABLE IX. Magnetic Data for $Mn(C_3H_4N_2)_4(NCS)_2$.

T (K)	μ_{eff} (B.M.)	X'_M(exp.) $\times 10^5$ (cgs emu)	X'_M(calcd) $\times 10^5$ (cgs emu)
93.2	6.06	4920	4903
103.1	6.05	4441	4450
113.1	6.07	4076	4073
123.1	6.08	3749	3755
133.1	6.09	3484	3484
143.1	6.04	3190	3248
153.1	6.18	3115	3043
163.1	6.11	2861	2862
173.1	6.09	2676	2701
183.1	6.06	2504	2558
193.1	6.15	2447	2429
203.1	6.13	2316	2312
213.1	6.11	2194	2206
223.1	6.17	2137	2109
233.1	6.16	2034	2021
243.1	6.12	1929	1939
253.1	6.22	1913	1864
263.2	6.14	1792	1795
273.2	6.11	1707	1730
283.2	6.14	1664	1670
293.2	6.18	1628	1614

frequencies [7b, 25]. The ν(CH) stretching frequencies of the ligand appear in the usual range 3150–3100 cm^{-1}. The weak or strong bands in the area 3050–2400 cm^{-1} in both spectra are assigned to combination and overtone bands of the organic ligand [25]. Typical is their weakening in the complex formation.

The very strong band at 2078 cm^{-1} in the complex spectrum is assigned to ν(CN) stretching band due to isothiocyanato ion NCS^- [26]. The ν(ring) stretching frequencies of pyrazole appear obviously in both spectra at 1800–1600 cm^{-1} [25]. The δ(ring) bending bands without making detailed assertment between them are observed in both spectra or only in the pyrazole spectrum at following areas 1560–1300, 1240–1220, 950–920 and 660–620 cm^{-1} [25].

The δ(CH) bending bands are also observed at several ranges. They are 1270–1250, 1070–1030, 900–880, 842 and 780–760 cm^{-1} [25]. The δ(NH) bending bands are assigned to 1160–1120 cm^{-1} in both spectra.

From viewpoint of the complex formation the most interesting bands appear under 800 cm^{-1}. The medium band at 870 cm^{-1} is assigned to ν(CS) stretching of the NCS^- ion [26]. The ν(M–NCS) stretching vibrations appear in the complex spectrum most probably at 797 and 720–670 cm^{-1} [26]. The ν(M–N) stretching vibrations (which may be due to interactions between the metal and pyrazole or NCS^-) are assigned to strong bands at 600–540 [26] and 240 cm^{-1} [26, 27]. The δ(NCS) bending vibration is obviously recognized at 480 cm^{-1} [26a, 27].

The reflectance spectrum of the complex in paraffin oil appeared to be similar to that reported for $Mn(5\text{-}CH_3Hpz)_4(NO_3)_2$ [28]. It showed only one very weak band at 23 260 cm^{-1} (430 nm) which is suggested to be due to the transition $^6A_{1g} \rightarrow {}^4T_{2g}$ [29]. After this the first band at 18 000–20 000

TABLE X. Observed Infrared Bands (cm^{-1}) of Pyrazole and $Mn(C_3H_4N_2)_4(NCS)_2$ Complex and their Assignments.

Pyrazole	Complex	Assignment[a]	Pyrazole	Complex	Assignment[a]
	3430s[b]	ν(NH)	1153vs	1160vs	δ(NH), δ(NH)
	3320vs	ν(NH)	1140vs	1135vs	δ(NH), δ(NH)
3150vsb	3140w	ν(CH), ν(CH)		1125vs	δ(NH)
	3120s	ν(CH), ν(CH)	1059vs	1063vs	δ(CH), δ(CH)
3050vs	3050vw	c. and o.	1037vs	1047vs	δ(CH), δ(CH)
2980vs	2980w	c. and o.	943vs	947vs	δ(ring), δ(ring)
	2920vw	c. and o.	930vs		δ(ring),
2810sh	2845w	c. and o.	922vs	917vs	δ(ring), δ(ring)
2700sh	2710vw	c. and o.	896vs	893m	δ(CH), δ(CH)
2605s	2580vw	c. and o.	880vs		δ(CH),
2490sh		c.		870m	ν(CS)
2395w		c.	842vs		δ(CH)
2070w	2078vs	ν(ring), ν(CN)		797vs	ν(M–NCS)
1765w	1755w	ν(ring), ν(ring)	773vs		δ(CH)
1730m		ν(ring)	763vs	766vs	δ(CH), δ(CH)
1630m	1620vw	ν(ring), ν(ring)		720vs	ν(M–NCS)
1553m		δ(ring), δ(ring)		695vs	ν(M–NCS)
1533m	1530s	δ(ring), δ(ring)		677vs	ν(M–NCS)
1467s	1472s	δ(ring), δ(ring)	654m		δ(ring)
1398vs	1407vs	δ(ring), δ(ring)	623vs	635vw	δ(ring), δ(ring)
1361vs	1357vs	δ(ring), δ(ring)		597s	ν(M–N)
	1315vw	δ(ring), δ(ring)		587s	ν(M–N)
1265m	1267m	δ(CH), δ(CH)		548m	ν(M–N)
1256m	1253w	δ(CH), δ(CH		480m	δ(NCS)
1233sh		δ(ring)		240s	ν(M–N)
1227w		δ(ring)			

[a] SCN^- (KSCN) bands: 2805m, 2060vs, 974s, 955m, 753vs, 491vs, 476s. [b] b = broad, m = medium, s = strong, sh = shoulder, v = very, w = weak. ν = stretching, δ = bending, c. = combination, o. = overtones.

TABLE XI. TG Data for $Mn(C_3H_4N_2)_4(NCS)_2$.

Process	Temperature range (K)	Residue (% from total) Found	Calculated
$Mn(C_3H_4N_2)_4(NCS)_2$			
$\downarrow -2C_3H_4N_2$	363–437		
$Mn(C_3H_4N_2)_2(NCS)_2$		69.7	69.3
$\downarrow -2C_3H_4N_2$	437–570		
$Mn(NCS)_2$		40.2	38.6
$\downarrow -(CN)_2$	581–750		
$MnS_2(\rightarrow\alpha\text{-MnS} + S)$	750→	27.1	26.9

cm^{-1} due to the transition $^6A_{1g} \rightarrow {}^4T_{1g}$ has been flattened to unobservable and the other bands characteristic for Mn(II) complexes were melted to one showing continuously increasing absorption at shorter wavelengths (>25 000 cm^{-1}).

Thermal Properties

The TG curve of the complex in dynamic nitrogen atmosphere is shown in Fig. 4 and the thermal processes elucidated from it in Table XI. The compound is shown to be stable to 363 K, after which it leaves first two pyrazole molecules to 437 K. These pyrazole molecules are obviously those unstacked in the *c*-direction and containing the N(3) and N(3)^i nitrogen atoms. Presumably the difference in the strength of the two intermolecular hydrogen bonds is the reason for the thermal escape of the N(3) pyrazole molecules first from the complex. These conclusions are also in accord to the anisotropic temperature factors (Table III and Fig. 1), which show the temperature vibrations of the atoms of the N(3) pyrazole rings to be considerably stronger than those of the N(1) pyrazole rings.

In the next step the last two pyrazole molecules escape between 437 and 570 K. Finally the left $Mn(NCS)_2$ decomposes to MnS_2 from 581 to 750 K.

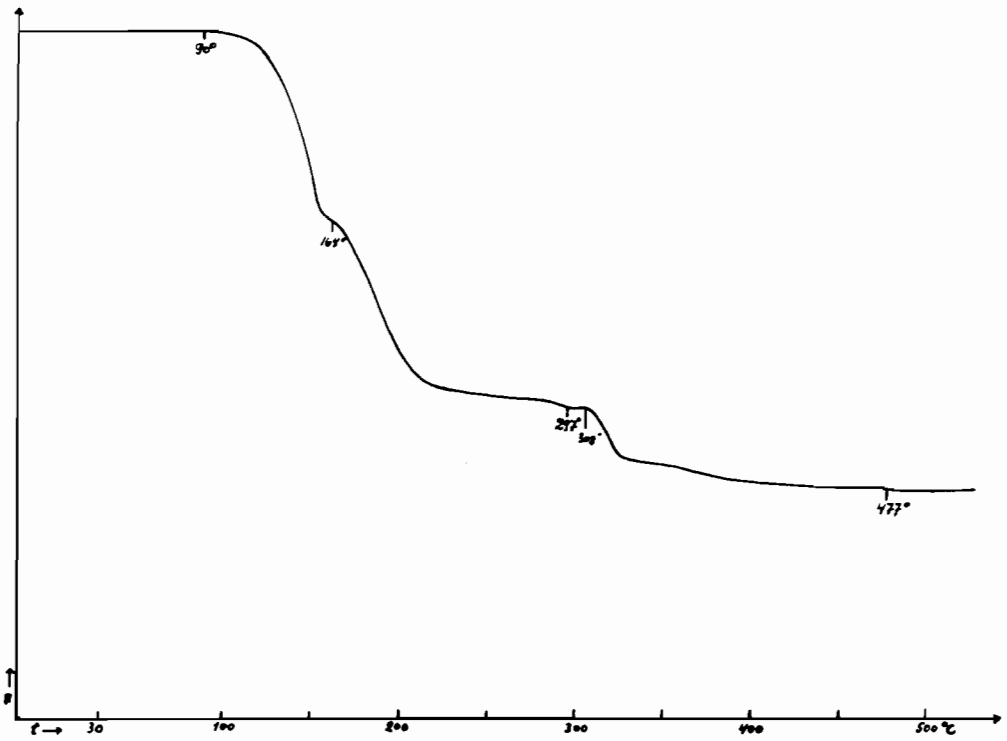

Fig. 4. TG curve of $Mn(C_3H_4N_2)_4(NCS)_2$ in dynamic N_2 atmosphere.

At higher temperatures MnS_2 obviously decomposes to sulphur and α-MnS [30].

The escape of the pyrazole molecules in two stages points to two different metal-bonded ligand groups, in agreement with what has been presented in the foregoing discussion.

$M(Hpz)_4SO_4$ complexes, where M = Co, Cu, Zn or Cd, have also been shown to give up the pyrazole ligands in one or several stages beginning between 353 and 433 K [31].

References

1 S. Trofimenko, *Chem. Rev., 72,* 497 (1972).
2 T. R. Musgrave and E. R. Humburg, Jr., *J. Inorg. Nucl. Chem., 32,* 2229 (1970).
3 R. J. Sundberg and R. B. Martin, *Chem. Rev., 74,* 471 (1974).
4 S. Martinez-Carrera, *Acta Cryst., 20,* 783 (1966).
5 a) B. F. Fieselmann and G. D. Stucky, *Inorg. Chem., 17,* 2074 (1978). b) R. Usón, L. A. Oro, M. A. Ciriano, M. T. Pinillos, A. Tiripicchio and M. Tiripicchio Camellini, *J. Organomet. Chem., 205,* 247 (1981).
6 J. Reedijk and J. A. Smit, *Rec. Trav. Chim., 90,* 1135 (1971).
7 a) J. Reedijk, B. A. Stork-Blaisse and G. C. Verschoor, *Inorg. Chem., 10,* 2594 (1971). b) S. Gorter, A. D. van Ingen Schenau and G. C. Verschoor, *Acta Cryst., B 30,* 1867 (1974).
8 A. I. Vogel, 'Quantitative Inorganic Analysis', 3rd Edition, Longmans, London, 1961, pp. 434 and 569.
9 D. N. Batchelder and R. O. Simmons, *J. Chem. Physics, 41,* 2324 (1964).
10 D. T. Cromer and J. B. Mann, *Acta Cryst., A 24,* 321 (1968).
11 'International Tables for X-ray Crystallography', Vol. IV, Kynoch Press, Birmingham, 1974.
12 J. M. Stewart, 'The XRAY system-version of 1976. Tech. Rep. TR-446'. Computer Science Center, Univ. of Maryland, College Park, Maryland, U.S.A.
13 a) M. R. Truter and B. L. Vickery, *J. Appl. Cryst., 6,* 323 (1973), Program No. 124. b) P. E. Werner, *Arkiv. Kemi, 31,* 513 (1970). P. E. Werner, *J. Appl. Cryst., 9,* 216 (1976).
14 B. N. Figgis and J. Lewis, in 'Technique of Inorganic Chemistry', Vol. 4, Eds. H. B. Jonassen and A. Weissberger, Intersc. Publ., London, 1965, p. 231.
15 C. K. Johnson, ORTEP (1965), Report ORNL-3794. Oak Ridge National Laboratory, Tennessee, U.S.A.
16 W.C. Hamilton, *Acta Cryst., 12,* 609 (1959).
17 A. J. Finney, M. A. Hitchman, C. L. Raston, G. L. Rowbottom, B. W. Skelton and A. H. White, *Aust. J. Chem., 34,* 2095 (1981).
18 C. W. Reimann, A. D. Mighell and F. A. Mauer, *Acta Cryst., 23,* 135 (1967).
19 A. D. Mighell, C. W. Reimann and A. Santoro, *Acta Cryst., B 25,* 595 (1969).
20 C. W. Reimann, A. Santoro and A. D. Mighell, *Acta Cryst., B 26,* 521 (1970).
21 A. M. G. D. Rodrigues, Y. P. Mascarenhas and M. M. Rodrigues, *Acta Cryst., B 36,* 159 (1980).
22 A. Mighell, A. Santoro, E. Prince and C. Reimann, *Acta Cryst., B 31,* 2479 (1975).
23 T. La Cour and S. E. Rasmussen, *Acta Chem. Scand., 27,* 1845 (1973).

24 A. Weiss and H. Witte, 'Magnetochemie, Grundlagen und Anwendungen', Verlag Chemie, Weinheim, 1973.
25 A. Zecchina, L. Cerruti, S. Coluccia and E. Borello, *J. Chem. Soc., (B),* 1363 (1967).
26 a) K. Nakamoto, 'Infrared and Raman Spectra of Inorganic and Coordination Compounds', 3rd Ed., Wiley & Sons, New York, 1978, pp. 215, 270–274 and 379. b) H. Siebert, 'Anwendungen der Schwingungsspektroskopie in der anorganischen Chemie', Springer-Verlag, Berlin, 1966, pp. 155–56. c) A. H. Norbury, *Adv. Inorg. Chem. and Radiochem., 17,* 231 (1975).
27 A. Sabatini and I. Bertini, *Inorg. Chem., 4,* 959 (1965).
28 J. Reedijk, *Rec. Trav. Chim., 89,* 993 (1970).
29 a) H. L. Schläfer and G. Gliemann, 'Einführung in die Ligandenfeldtheorie', Akadem. Verlagsgesellschaft, Frankfurt am Main, 1967, pp. 52 and 98. b) C. J. Ballhausen, 'Introduction to Ligand Field Theory', McGraw-Hill, London, 1962, p. 245.
30 a) S. Furuseth and A. Kjekshus, *Acta Chem. Scand., 19,* 1405 (1965). b) M. Avinor and G. De Pasquali, *J. Inorg. Nucl. Chem., 32,* 3403 (1970).
31 A. Anagnostopoulos, D Nicholls and K. R. Seddon, *J. Inorg. Nucl. Chem., 36,* 2235 (1974).